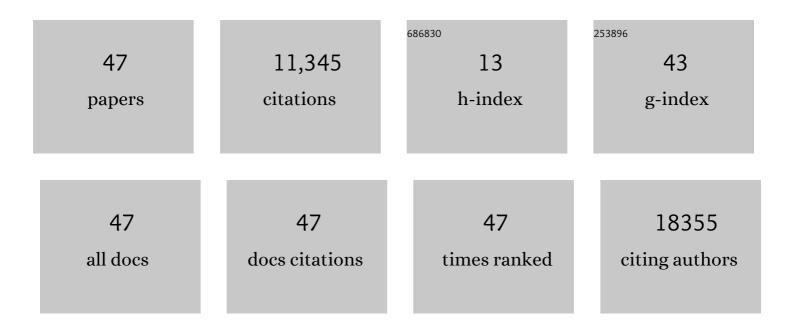
Milan Mazur

List of Publications by Year in descending order

Source: https://exaly.com/author-pdf/2171388/publications.pdf Version: 2024-02-01



#	ARTICLE	IF	CITATIONS
1	In vitro biological activity of copper(II) complexes with NSAIDs and nicotinamide: Characterization, DNA- and BSA-interaction study and anticancer activity. Journal of Inorganic Biochemistry, 2022, 228, 111696.	1.5	16
2	Synthesis, Spectroscopic Properties and Hirshfeld Surface Analysis of 3,14-Dimethyl-2,6,13,17-tetraazoniatricyclo(16.4.0.07,12)docosane Tetrachloride Tetrahydrate. Asian Journal of Chemistry, 2021, 33, 1861-1867.	0.1	0
3	Structural characterization, spectroscopic properties, and Hirshfeld surface analysis of two copper(II) complexes with 3,14-dimethyl and 3,14-diethyl-2,6,13,17-diazadiazoniatricyclo[16.4.0.07,12]docosa-2,13-diene. Journal of Molecular Structure, 2021, 1231, 129897.	1.8	2
4	A variable-temperature Q- and X-band EPR study of spin-crossover iron(III) Schiff base complex. Chemical Papers, 2020, 74, 3683-3692.	1.0	1
5	Hydrogen bonding supramolecular networks of copper(II) 2-choronicotinate complexes with picolinamide, nicotinamide, N-methyl-nicotinamide, 2-pyridylmethanol and 4-pyridylmethanol: Hirshfeld surface analysis and spectral properties. Chemical Papers, 2020, 74, 3727-3740.	1.0	1
6	Synthesis, crystal structure, and spectroscopic properties of bis(rac-5,5,7,12,12,14-hexamethyl-1,4,8,11-tetraazacyclotetradecane)(μ-1,2,3,4-oxalato)dichloridozincate(II)(μ tetrachloridozincate monohydrate. Journal of Molecular Structure, 2020, 1221, 128711.	4- 1,8 ,3-oxa	alæto)dichron
7	Synthesis, Crystal Structure, Spectroscopic Properties, and Hirshfeld Surface Analysis of Diaqua [3,14-dimethyl-2,6,13,17 tetraazatricyclo(16.4.0.07,12)docosane]copper(II) Dibromide. Crystals, 2019, 9, 336.	1.0	9
8	Impact of the Schiff base ligand substituents on the solid state and solution properties of eleven iron(<scp>iii</scp>) complexes. New Journal of Chemistry, 2019, 43, 13916-13928.	1.4	7
9	Synthesis, structural characterization, EPR spectroscopy and Hirshfeld surface analysis of a novel Cu ²⁺ -doped 3,14-diethyl-2,13-diaza-6,17-diazoniatricyclo[16.4.0.0 ^{7,12}]docosane bis(perchlorate). Acta Crystallographica Section C, Structural Chemistry, 2019, 75, 616-622.	0.2	6
10	High‣pin Mononuclear Iron(III) Complexes with Pentadentate Schiff Base Ligands: Structural Analysis and Magnetic Properties. ChemPlusChem, 2019, 84, 358-367.	1.3	9
11	Crystal structures and spectroscopic properties of copper(II)–dipicolinate complexes with benzimidazole ligands. Transition Metal Chemistry, 2018, 43, 507-516.	0.7	1
12	Impact of Substituent Variation on the Presence of Thermal Spin Crossover in a Series of Mononuclear Iron(III) Schiff Base Complexes with Terminal Pseudohalido Coâ€ligands. Chemistry - A European Journal, 2018, 24, 5191-5203.	1.7	15
13	Copper(II) Thiosemicarbazone Complexes and Their Proligands upon UVA Irradiation: An EPR and Spectrophotometric Steady-State Study. Molecules, 2018, 23, 721.	1.7	11
14	Nitrosalicylatocopper(II) complexes with chelating pyridine derivatives. Acta Chimica Slovaca, 2018, 11, 21-25.	0.5	3
15	A systematic study of the hydration and drying process of silica xerogels using Cu(II) EPR spectroscopy. Journal of Sol-Gel Science and Technology, 2017, 82, 855-861.	1.1	0
16	Synthesis, Crystal Structure and Spectral Properties of Copper(II) 2-Chloronicotinato Complexes with N-Heterocyclic Ligands. Nova Biotechnologica Et Chimica, 2016, 15, 190-199.	0.1	2
17	â€~U-spectrum' type of Gd(III) EPR spectra recorded at various stages of TEOS-based sol–gel process. Journal of Sol-Gel Science and Technology, 2016, 79, 220-227.	1.1	5
18	Monitoring the Tetraethyl Orthosilicate (TEOS)-Based Sol–Gel Process with Cu(II) Ions as a Spin Probe. Applied Magnetic Resonance, 2016, 47, 1-12.	0.6	14

Milan Mazur

#	Article	IF	CITATIONS
19	Tetraethyl orthosilicate (TEOS)-based sol–gel process monitored by EPR spectroscopy with VO(II) cations as a spin-probe. Journal of Sol-Gel Science and Technology, 2015, 76, 110-119.	1.1	4
20	EPR Spectroscopy of a Clinically Active (1:2) Copper(II)-Histidine Complex Used in the Treatment of Menkes Disease: A Fourier Transform Analysis of a Fluid CW-EPR Spectrum. Molecules, 2014, 19, 980-991.	1.7	27
21	Unusual EPR Spectra with Inverse Axial g values of Chlorosalicylate–Cu(II)–2,6-Pyridinedimethanol Complex in Frozen Water–Methanol Solution. Applied Magnetic Resonance, 2013, 44, 571-582.	0.6	12
22	Investigation of 3,5-dichlorosalicylate-copper(II)-(3-pyridylmethanol or N,N′-diethylnicotinamide) complex systems by EPR spectroscopy. Chemical Papers, 2013, 67, .	1.0	0
23	3-Pyridylmethanol vs. N,N′-diethylnicotinamide in copper(II) complex formation – A comparative EPR study. Journal of Molecular Structure, 2013, 1049, 41-47.	1.8	2
24	Methyl- and methoxysalicylatocopper complexes with 2-pyridylmethanol: Synthesis, spectral properties, structure and EPR characterization in solid-state and in solution. Open Chemistry, 2012, 10, 1506-1515.	1.0	4
25	Hydrogenâ€Bondâ€Based Magnetic Exchange Between μâ€Diethylnicotinamide(aqua)bis(Xâ€salicylato)copper(Polymeric Chains. Zeitschrift Fur Anorganische Und Allgemeine Chemie, 2011, 637, 224-231.	(II) 0.6	3
26	Synthesis, properties and crystal structures of nitrobenzoatocopper(II) complexes with pyrazinecarboxamide. Transition Metal Chemistry, 2011, 36, 883-889.	0.7	2
27	EPR Study of 5-Chlorosalicylate-Cu(II)-N,N-Diethylnicotinamide Ternary Complex Systems in Frozen Water–Methanol Solutions. Applied Magnetic Resonance, 2011, 40, 405-411.	0.6	4
28	EPR Study of 5-Chlorosalicylate-Cu(II)-3-Pyridylmethanol Ternary Complex Systems in Frozen Water–Methanol Solutions. Applied Magnetic Resonance, 2010, 39, 423-435.	0.6	6
29	Self-Assembled Hydrogen-Bonding Chains of Copper(II) 2-Nitrobenzoate with Nicotinamide. Journal of Chemical Crystallography, 2010, 40, 179-184.	0.5	13
30	[Cu(X-salicylato)2(N,N-diethylnicotinamide)2(H2O)2] complexes: conformational polymorphism and its consequence in supramolecular hydrogen-bonding networks formation. Structural Chemistry, 2010, 21, 1093-1102.	1.0	11
31	Oneâ€Dimensional and Twoâ€Dimensional Coordination Polymers of Copper(II) Nitrobenzoate with Bridging 3â€Pyridylmethanol Ligand. Zeitschrift Fur Anorganische Und Allgemeine Chemie, 2010, 636, 589-594.	0.6	4
32	Free radicals and antioxidants in normal physiological functions and human disease. International Journal of Biochemistry and Cell Biology, 2007, 39, 44-84.	1.2	10,891
33	A dozen useful tips on how to minimise the influence of sources of error in quantitative electron paramagnetic resonance (EPR) spectroscopy—A review. Analytica Chimica Acta, 2006, 561, 1-15.	2.6	31
34	Structural diversity of coordination polymers with bridging 3-pyridylmethanol ligand: New type of coordination polymer with different stereochemistry of copper(II) atom. Polyhedron, 2006, 25, 1561-1566.	1.0	28
35	Analysis of the longitudinal, "sloping plateau―effect of a planar sample in a single TE102 rectangular electron paramagnetic resonance cavity. Analytica Chimica Acta, 2005, 538, 165-174.	2.6	2
36	Spectral properties and bio-activity of copper(II) clofibriates, part III: crystal structure of Cu(clofibriate)2(2-pyridylmethanol)2, Cu(clofibriate)2(4-pyridylmethanol)2(H2O) dihydrate, and Cu2(clofibriate)4(N,N-diethylnicotinamide)2. Inorganica Chimica Acta, 2004, 357, 3211-3222.	1.2	45

Milan Mazur

#	Article	IF	CITATIONS
37	Analysis of the radial and longitudinal effects of a planar sample in a single TE102 rectangular electron paramagnetic resonance (EPR) cavity. Analytica Chimica Acta, 2004, 526, 163-176.	2.6	3
38	Influence of the variable wall thickness of the sample tubes and a quartz Dewar on the EPR signal intensity in a single TE102 and double TE104 rectangular cavity. Analytica Chimica Acta, 2003, 482, 229-248.	2.6	8
39	From a point-like to an arbitrarily shaped sample. Analytica Chimica Acta, 2002, 456, 129-146.	2.6	7
40	Radial and longitudinal profiles of the electron paramagnetic resonance signal intensity of a single TE102 rectangular cavity. Analytica Chimica Acta, 2002, 464, 163-170.	2.6	3
41	Influence of the movement of "over full-length cavity―cylindrical samples along the x-axis of a double TE104 and a single TE102 rectangular cavity on the electron paramagnetic resonance. Analytica Chimica Acta, 2001, 443, 127-141.	2.6	6
42	Analysis of the Radial and Longitudinal Effect in a Double TE104 and a Single TE102 Rectangular Cavity. Journal of Magnetic Resonance, 2000, 142, 37-56.	1.2	24
43	Electron paramagnetic resonance signal intensity of a line-like sample with a variable length situated at an arbitrary position along the common sample-cavity axis. Theoretical prediction versus experimental measurement. Analytica Chimica Acta, 1998, 367, 233-243.	2.6	11
44	Analysis of the Movement of Line-like Samples of Variable Length along theX-Axis of a Double TE104and a Single TE102Rectangular Cavity. Journal of Magnetic Resonance, 1997, 129, 188-200.	1.2	31
45	Quantitative electron paramagnetic resonance (EPR) spectrometry with a TE104 double rectangular cavity Part 1. A simple alignment procedure for the precision positioning of the sample. Analytica Chimica Acta, 1996, 333, 249-252.	2.6	25
46	Quantitative electron paramagnetic resonance (EPR) spectrometry with a TE104 double rectangular cavity Part 2. Analysis of sample and TE104 cavity error sources associated with the movement of line-like samples into the TE104 cavity. Analytica Chimica Acta, 1996, 333, 253-265.	2.6	26
47	Mn2+ EPR investigation of sol-gel process in silica xerogels at 77 K. Physica B: Condensed Matter, 1995, 210, 55-58.	1.3	8